

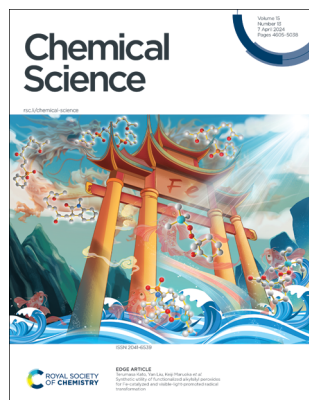
Chemical Science

rsc.li/chemical-science

The Royal Society of Chemistry is the world's leading chemistry community. Through our high impact journals and publications we connect the world with the chemical sciences and invest the profits back into the chemistry community.

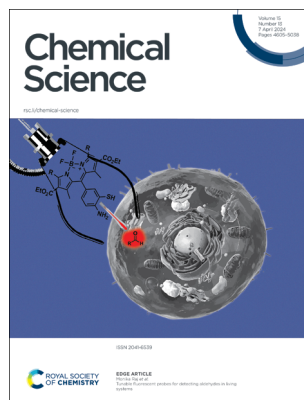
IN THIS ISSUE

ISSN 2041-6539 CODEN CSHCBM 15(13) 4605–5038 (2024)



Cover

See Terumasa Kato, Yan Liu, Keiji Maruoka *et al.*, pp. 4757–4762. Image reproduced by permission of Keiji Maruoka from *Chem. Sci.*, 2024, **15**, 4757.



Inside cover

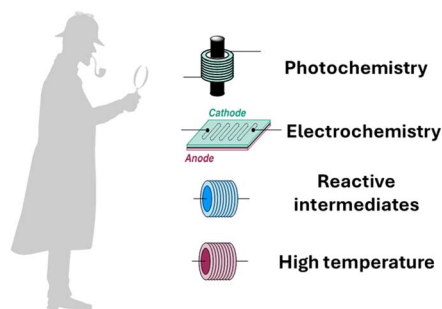
See Monika Raj *et al.*, pp. 4763–4769. Image reproduced by permission of Monika Raj from *Chem. Sci.*, 2024, **15**, 4763.

PERSPECTIVE

4618

Continuous flow synthesis enabling reaction discovery

Antonella Ilenia Alfano, Jorge García-Lacuna, Oliver M. Griffiths, Steven V. Ley* and Marcus Baumann*

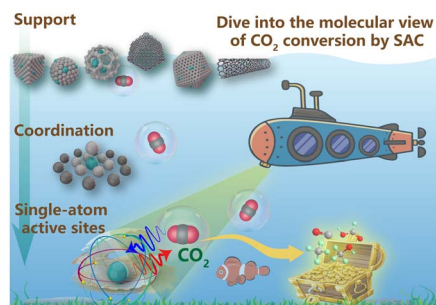


REVIEWS

4631

A molecular view of single-atom catalysis toward carbon dioxide conversion

Xin Shang, Xiaofeng Yang, Guodong Liu, Tianyu Zhang* and Xiong Su*



Environmental Science journals

One impactful portfolio for
every exceptional mind

Harnessing the power of interdisciplinary
science to preserve our environment

rsc.li/envsci

Fundamental questions
Elemental answers

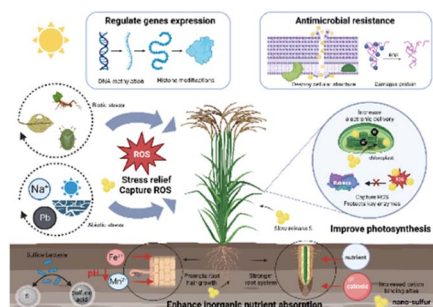


REVIEWS

4709

Unlocking the potential of nanoscale sulfur in sustainable agriculture

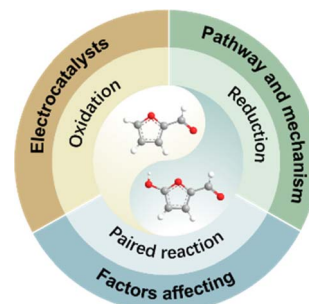
Yi Sun, Yaqi Jiang, Yuanbo Li, Qibin Wang, Guikai Zhu, Tianjing Yi, Quanlong Wang, Yi Wang, Om Parkash Dhankher, Zhiqiang Tan, Iseult Lynch, Jason C. White,* Yukui Rui* and Peng Zhang*



4723

Electrocatalytic conversion of biomass-derived furan compounds: mechanisms, catalysts and perspectives

Peipei Zhu,* Mingzhu Shi, Zhipeng Shen, Xunfan Liao and Yiwang Chen*

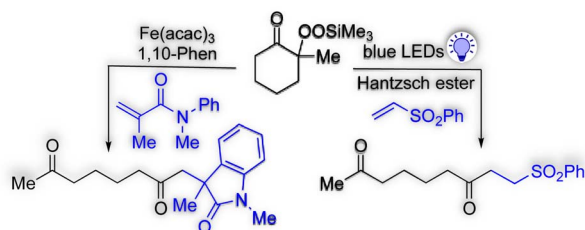


EDGE ARTICLES

4757

Synthetic utility of functionalized alkylsilyl peroxides for Fe-catalyzed and visible-light-promoted radical transformation

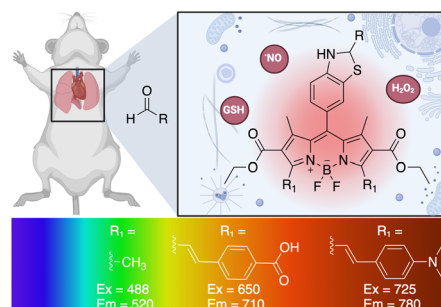
Jiahao Liu, Shiyong Liu, Zhe Wang, Terumasa Kato,* Yan Liu* and Keiji Maruoka*



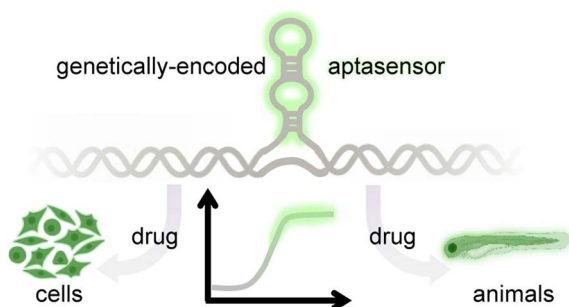
4763

Tunable fluorescent probes for detecting aldehydes in living systems

Rachel Wills, Rajendra Shirke, Hannah Hrnecir, John M. Talbott, Kirti Sad, Jennifer M. Spangle, Adam D. Gracz and Monika Raj*



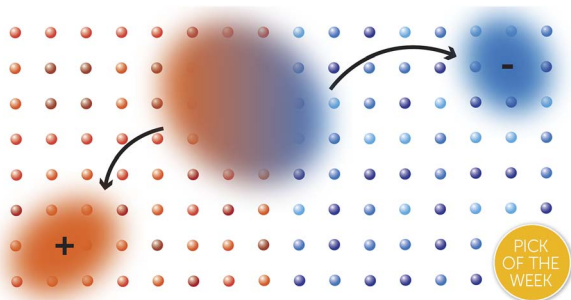
4770



Non-invasive single cell aptasensing in live cells and animals

Eiman A. Osman, Thomas P. Rynes, Y. Lucia Wang, Karen Mruk and Maureen McKeague*

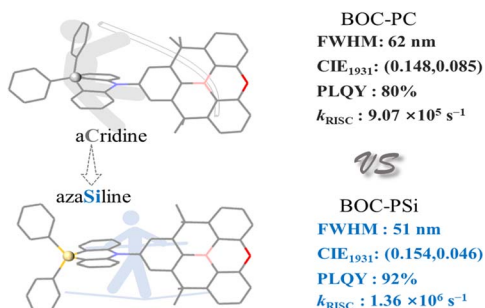
4779



Delocalisation enables efficient charge generation in organic photovoltaics, even with little to no energetic offset

Daniel Balzer and Ivan Kassal*

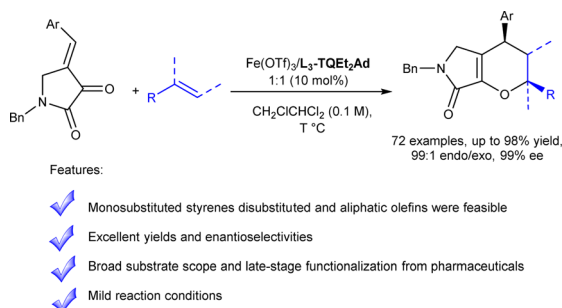
4790



Realizing highly efficient deep-blue organic light-emitting diodes towards Rec.2020 chromaticity by restricting the vibration of the molecular framework

Chuan Li, Kai Zhang, Yanju Luo, Yang Yang, Yong Huang, Mengjiao Jia, Yuling He, Yue Lei, Jian-Xin Tang,* Yan Huang and Zhiyun Lu*

4797



Iron^{III}-catalyzed asymmetric inverse-electron-demand hetero-Diels-Alder reaction of dioxypyrrolidines with simple olefins

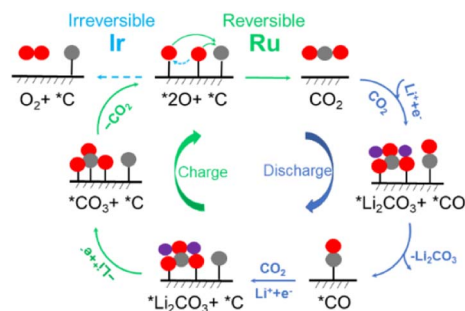
Tangyu Zhan, Liang Zhou, Yuqiao Zhou, Bingqian Yang, Xiaoming Feng* and Xiaohua Liu*



4804

Reversible and irreversible reaction mechanisms of Li-CO₂ batteries

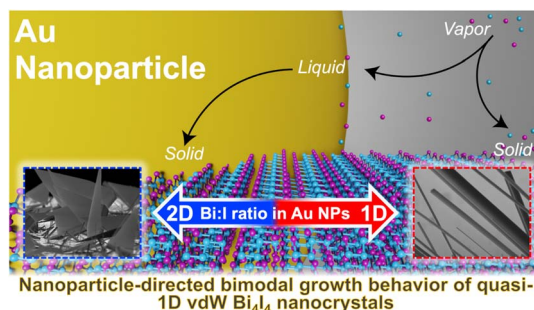
Xinxin Zhang, Yu Wang* and Yafei Li*



4811

Nanoparticle-directed bimodal crystallization of the quasi-1D van der Waals phase, Bi₄I₄

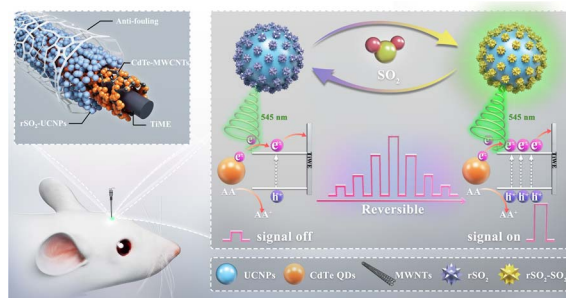
Steven Jay Allison, Dmitri Leo Mesoza Cordova, Maham Hasib, Toshihiro Aoki and Maxx Q. Arguilla*



4824

A reversible photoelectrochemical microsensor for dynamically monitoring sulfur dioxide in the epileptic brain

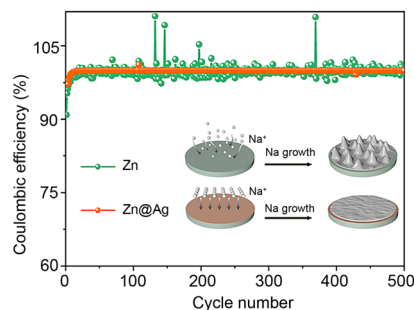
Danying Lin, Tao Lu, Xiao Wang, Xiaoxue Ye* and Zhihong Liu*



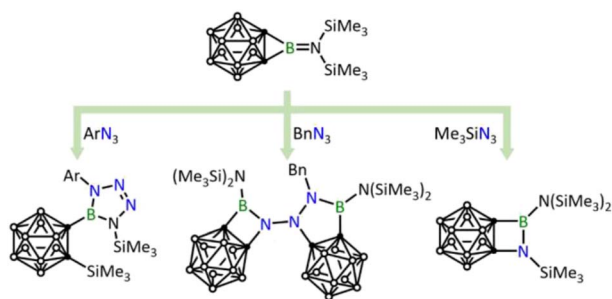
4833

A conductive and sodiophilic Ag coating layer regulating Na deposition behaviors for highly reversible sodium metal batteries

Xiaomin Chen, Xunzhu Zhou, Zhuo Yang, Zhiqiang Hao, Jian Chen, Wenxi Kuang, Xiaoyan Shi, Xingqiao Wu, Lin Li* and Shu-Lei Chou*



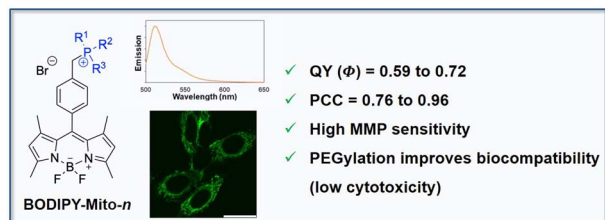
4839



Avenue to novel o-carboranyl boron compounds – reactivity study of o-carborane-fused aminoborirane towards organic azides

Junyi Wang, Libo Xiang, Xiaocui Liu, Alexander Matler, Zhenyang Lin* and Qing Ye*

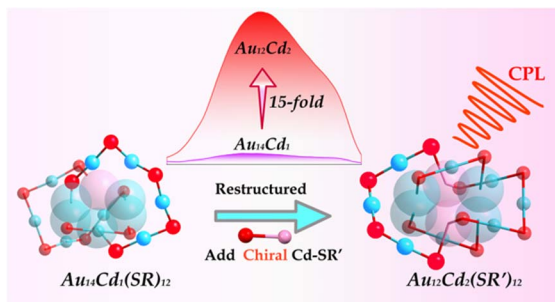
4846



Mitochondria-targeting biocompatible fluorescent BODIPY probes

Edward R. H. Walter, Lawrence Cho-Cheung Lee, Peter Kam-Keung Leung, Kenneth Kam-Wing Lo* and Nicholas J. Long*

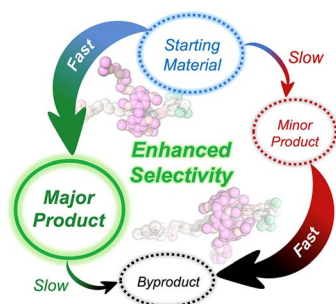
4853



Construction of an Au₁₂Cd₂ nanocluster with circularly polarized luminescence by a metal- and ligand-exchange strategy

Jun Zhou, Xiaofei Yang, Peisen Zheng, Qinzhen Li, Xiaowu Li, Jinsong Chai, Baoyu Huang,* Sha Yang* and Manzhou Zhu*

4860



Kinetically controlled synthesis of rotaxane geometric isomers

Dillon R. McCarthy, Ke Xu, Mica E. Schenkelberg, Nils A. N. Balemire, Huiming Liang, Shea A. Bellino, Jianing Li and Severin T. Schneebeli*



Metadynamics simulations reveal alloying-dealloying processes for bimetallic PdGa nanoparticles under CO₂ hydrogenation

Simultaneously enhancing organic phosphorescence quantum yields and lifetimes for triphenylphosphine salt doped polymer films

Figure 1 consists of three main parts. The top part is an energy level diagram showing the potential energy surfaces for the singlet (S_0 , S_1) and triplet (T_1) states. The diagram illustrates the Intersystem Crossing (ISC) from S_1 to T_1 , the Thermally Activated Singlet-Triplet Crossing (TSTCT) from T_1 to S_1 , and the Thermally Activated Triplet-Triplet Crossing (TTET) from T_1 to T_1 . The middle part shows the chemical structure of NP-4Cz, a dendritic molecule with a bromine atom and a phosphine group. The bottom left is a graph of Photoluminescence Quantum Yield (%) vs Time (ns) for NP-4Cz and NP-3Cz-Cz. The bottom right is a series of fluorescence images of NP-4Cz in THF under UV on and UV off conditions at 1s, 2s, 3s, 4s, 5s, and 6s.

Energy level diagram showing the singlet (S_0 , S_1) and triplet (T_1) states. The diagram illustrates the Intersystem Crossing (ISC) from S_1 to T_1 , the Thermally Activated Singlet-Triplet Crossing (TSTCT) from T_1 to S_1 , and the Thermally Activated Triplet-Triplet Crossing (TTET) from T_1 to T_1 .


Chemical structure of NP-4Cz, a dendritic molecule with a bromine atom and a phosphine group.


Graph of Photoluminescence Quantum Yield (%) vs Time (ns) for NP-4Cz and NP-3Cz-Cz. The data shows that NP-4Cz has a higher quantum yield than NP-3Cz-Cz.


Fluorescence images of NP-4Cz in THF under UV on and UV off conditions at 1s, 2s, 3s, 4s, 5s, and 6s. The images show that the fluorescence intensity of NP-4Cz increases over time under UV on conditions.

Three-component dicarbofunctionalization of allylamines *via* nucleopalladation pathway: unlocking vicinal and geminal selectivity

Three-component dicarboxylation


vicinal selectivity
R-X
Pd
> 50 examples, upto 96% yield


vicinal selectivity
R-X
Pd
> 50 examples, upto 96% yield


vicinal selectivity
R-X
Pd
> 50 examples, upto 96% yield

Tryptamine

✓ nucleopalladation strategy ✓ removable directing group ✓ bio-relevant scaffolds

Bisindole

Differentiable simulation to develop molecular dynamics force fields for disordered proteins

Simulate 5 ns with Langevin dynamics using force field parameters \mathbf{F}

C_0, V_0 → Integrator time step using \mathbf{F} → C_1, V_1 → C_2, V_2 (5x10⁶ steps) → C_{n-1}, V_{n-1}

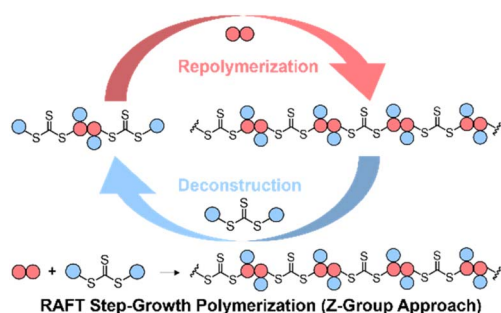
Automatic differentiation gets gradients of loss with respect to \mathbf{F} → Combine gradients over proteins, improve \mathbf{F}

from explicit solvent simulations → res-res distance μ and σ → KL divergence → Mean of $\ln(KL + 1)$ → Loss value

Simulation $R_g / \text{\AA}$ vs Experimental $R_g / \text{\AA}$

- G899dms (this work)
- P145Bonyhc + GBSNeck2
- a995B-disp + GBSNeck2
- a995B-disp explicit

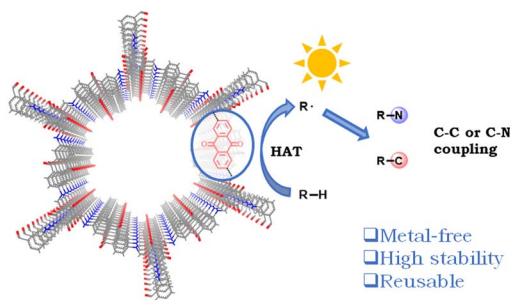
4910



RAFT step-growth polymerization via the Z-group approach and deconstruction by RAFT interchange

Jiajia Li, Joji Tanaka,* Qing Li, Claire Jing Jing Wang, Sergei Sheiko, Samantha Marie Clouthier, Jian Zhu and Wei You*

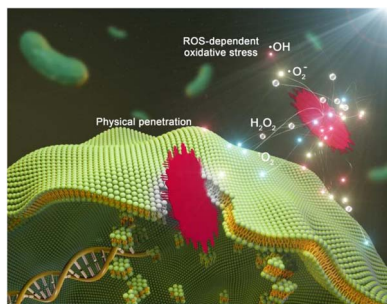
4920



Anthraquinone-based covalent organic framework as a recyclable direct hydrogen atom transfer photocatalyst for C-H functionalization

Zitong Wang, Pierce Yearry, Yingjie Fan and Wenbin Lin*

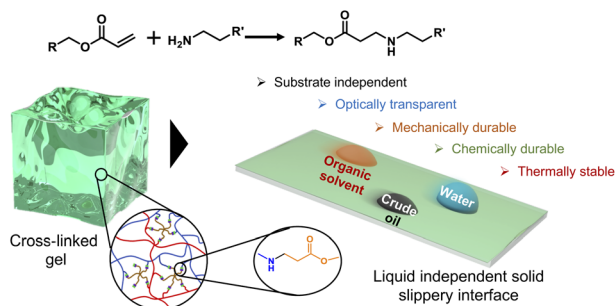
4926



Bacterial elimination via cell membrane penetration by violet phosphorene peripheral sub-nanoneedles combined with oxidative stress

Qiudi Shen, Jing Kang,* Xuwen Zhao, Wanqing Lou, Zhihao Li, Lihui Zhang, Bo Zhang, Jinying Zhang,* Bailiang Wang* and Alideertu Dong*

4938



Covalent crosslinking chemistry for controlled modulation of nanometric roughness and surface free energy

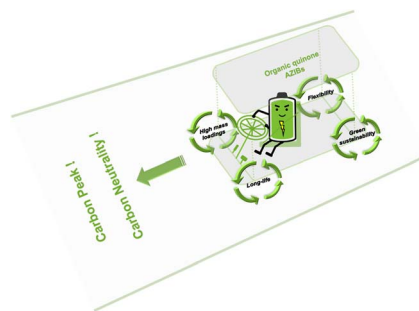
Debasmita Sarkar, Manideepa Dhar, Avijit Das, Sohini Mandal, Anirban Phukan and Uttam Manna*



4952

Constructing ultra-stable, high-energy, and flexible aqueous zinc-ion batteries using environment-friendly organic cathodes

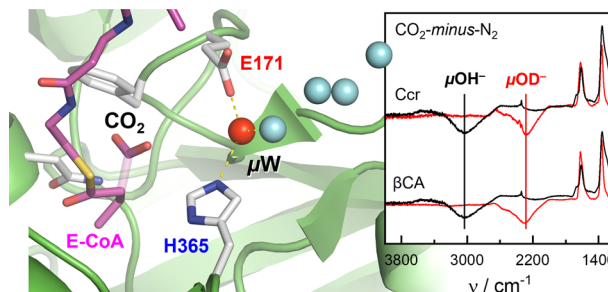
Chaojian Ding, Yonghui Wang, Chaobo Li, Jiawen Wang, Qichun Zhang* and Weiwei Huang*



4960

Infrared spectroscopy reveals metal-independent carbonic anhydrase activity in crotonyl-CoA carboxylase/reductase

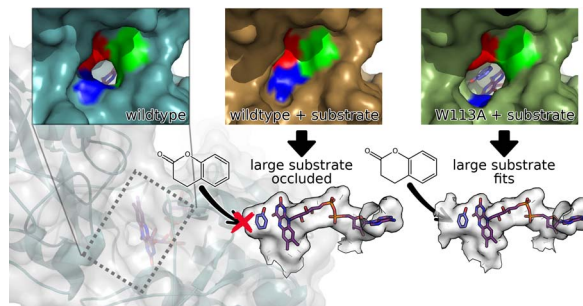
Aharon Gomez, Matthias Tinzi, Gabriele Stoffel, Hendrik Westedt, Helmut Grubmüller, Tobias J. Erb, Esteban Vöhringer-Martinez* and Sven T. Stripp*



4969

Rational design of a cyclohexanone dehydrogenase for enhanced α,β -desaturation and substrate specificity

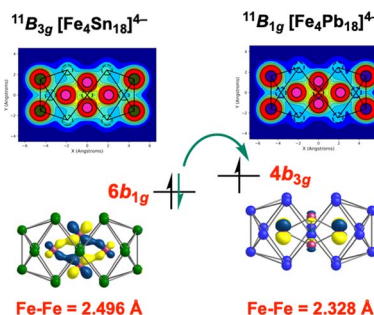
Warispreet Singh, Nicola L. Brown, Hannah V. McCue, Sophie R. Marriott, Richard C. Wilson, Justin Perry, Johan P. Turkenburg, Kshatresh D. Dubey, Stephen H. Prior, Andrew J. Carnell, Edward J. Taylor* and Gary W. Black*



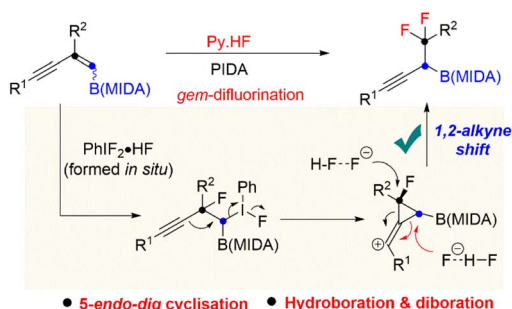
4981

Fe–Fe bonding in the rhombic Fe_4 cores of the Zintl clusters $[\text{Fe}_4\text{E}_{18}]^{4-}$ ($\text{E} = \text{Sn}$ and Pb)

Wei-Xing Chen, Zi-Sheng Li, Harry W. T. Morgan, Cong-Cong Shu, Zhong-Ming Sun* and John E. McGrady*



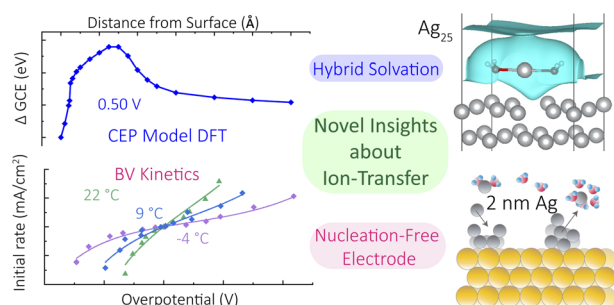
4989



Reactivity of 1,3-enyne MIDA boronates: exploration of novel 1,2-alkyne shift via *gem*-difluorination

Samir Manna, Debasis Aich, Subrata Hazra, Shivam Khandelwal and Santanu Panda*

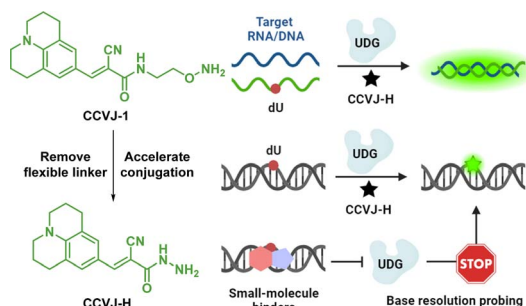
4996



Understanding ion-transfer reactions in silver electrodisolution and electrodeposition from first-principles calculations and experiments

Richard Kang,* Yang Zhao, Diptarka Hait, Joseph A. Gauthier, Paul A. Kempler, Kira A. Thurman, Shannon W. Boettcher* and Martin Head-Gordon*

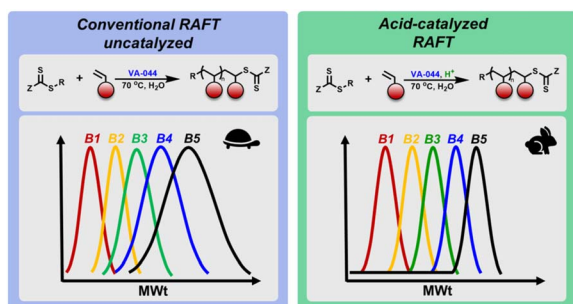
5009



Multifaceted nucleic acid probing with a rationally upgraded molecular rotor

Tuan-Khoa Kha, Qi Shi, Nirali Pandya and Ru-Yi Zhu*

5019



Enhanced synthesis of multiblock copolymers via acid-triggered RAFT polymerization

Maria-Nefeli Antonopoulou, Nghia P. Truong and Athina Anastasaki*



5027

Discovery of potent PROTAC degraders of Pin1 for the treatment of acute myeloid leukemia

Yunkai Shi, Minmin Liu, Mengna Li, Yiwen Mao, Jingkun Ma, Ruikai Long, Miaomiao Xu, Yaxi Yang, Wenlong Wang,* Yubo Zhou,* Jia Li* and Bing Zhou*

